JCTC Journal of Chemical Theory and Computation

Article

pubs.acs.org/JCTC

Cardiolipin Models for Molecular Simulations of Bacterial and Mitochondrial Membranes

Thomas Lemmin,[†] Christophe Bovigny,[†] Diane Lançon, and Matteo Dal Peraro*

Laboratory for Biomolecular Modeling, Institute of Bioengineering, School of Life Sciences, Ecole Polytechnique Fédérale de Lausanne (EPFL), CH-1015 Switzerland

Supporting Information

ABSTRACT: Present in bacterial and mitochondrial membranes, cardiolipins have a unique dimeric structure, which carries up to two charges (i.e., one per phosphate group) and, under physiological conditions, can be unprotonated or singly protonated. Exhaustive models and characterization of cardiolipins are to date scarce; therefore we propose an *ab initio* parametrization of cardiolipin species for molecular simulation consistent with commonly used force fields. Molecular dynamics simulations using these models indicate a protonation dependent lipid packing. A peculiar interaction with solvating mono- and divalent cations is also observed. The proposed models will contribute to the study of the assembly of more realistic bacterial and mitochondrial membranes and the investigation of the role of cardiolipins for the biophysical and biochemical properties of membranes and membrane-embedded proteins.

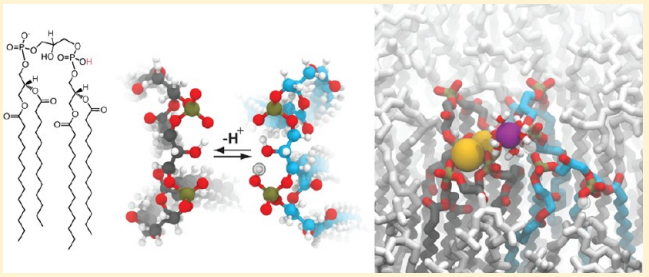

INTRODUCTION

The biological membrane constitutes an essential barrier for all living organisms. It is composed of a complex mixture of lipids and embedded proteins, forming a heterogeneous liquid-crystalline structure, organized into rafts of local association of lipids, with specific physicochemical properties.[1] Over the past years, it has been established that lipids do not constitute a simple structural support for proteins but interact, modify, and regulate their function.[2] Cells invest a substantial amount of energy to synthesize a large repertoire of different specific lipids, and nearly 5% of genes are involved in this synthesis.[3]

The composition of cell membranes in archaea, eukaryotes, and bacteria differ significantly. In particular, cardiolipins (CLs) are anionic phospholipids found in Gram-negative and Gram-positive bacteria, as well as in mitochondria and chloroplast inner membranes of eukaryotes. CLs are composed of two phosphatidyglycerol moieties connected by a single glycerol molecule (Figure 1). This dimeric structure is unique among phospholipids and confers an important role in the structural stabilization and activation membrane-dependent processes.[4] CLs can potentially carry two negative charges, one on each phosphate group (Figure 1C). Despite the apparent symmetry of the headgroup, the ionization of the phosphate groups occurs at different acidity levels ($pK_1 \sim 2.8$ and $pK_2 \sim 7.5$–9.5).[5] Under physiological conditions, CLs may therefore carry one negative charge. However, depending on the local pH and CL concentration, the deprotonation of both head groups cannot be excluded.[6] Importantly, cardiolipins have the tendency to produce high membrane curvature due to their large hydrophobic region and small charged head. Moreover, their bilayer and nonbilayer lipid properties are strongly modulated by the presence of divalent cations, namely, Mg^{2+} and Ca^{2+} ions.

Despite the importance of CLs in bacterial and mitochondrial membrane composition and their key role in cell division,[7] energy metabolism, and pathologies,[8] there are to date few molecular, biophysical, and biochemical characterizations thoroughly describing their properties and specific interactions with other lipid species and protein complexes.

Molecular simulations, at different levels of resolution, have contributed in many respects to describe the structural and kinetic properties of biological membranes in the past two decades.[9] Coarse-grained and united-atom models for cardiolipins have been parametrized.[10] Theses models provided useful mechanistic insights into phase transitions and aggregate geometries, but the lack of atomistic details inherent to a coarse-grained approach prevents a full molecular understanding of their properties. Similarly, united-atom models may suffer from the same limitations.[10a] Rog et al. proposed[11] the first all-atom OPLS-based models for the study of the mitochondrial inner membrane. Only the doubly charged protonation state was modeled in this case, and the partial charges were directly derived from Murzyn and Pasenkiewicz-Gierula and adapted from the OPLS force field.[12] They observed that the effect of CLs on the membrane properties is strongly dependent on the membrane composition and cannot be easily predicted. The interaction with cations, which is known to influence CL properties, however, has not yet been described. Recently, Aguayo et al.[10c] proposed a new hybrid set

Received: July 11, 2012

   dx.doi.org/10.1021/ct300590v | J. Chem. Theory Comput. XXXX, XXX, XXX–XXX

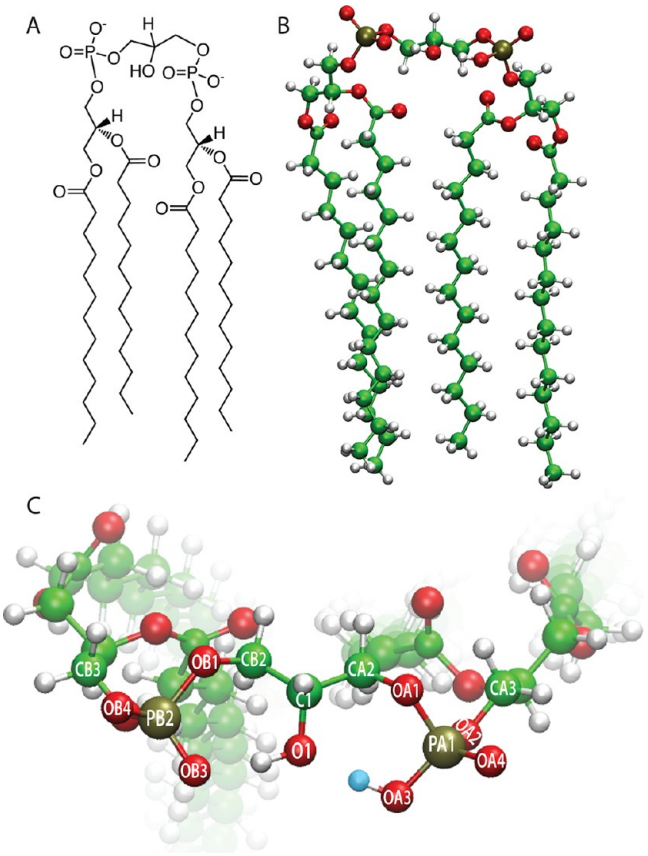

Figure 1. Cardiolipin structure and protonation states. Cardiolipin (CL) chemical structure (A) and 3D model (B). Cardiolipins form a unique dimeric phospholipid composed of four acyl tails. (C) CLs can be unprotonated (uCL) or singly protonated (pCL) depending on the protonation state of the OA3 oxygen atom, highlighted in blue. Relevant atom names composing the CL headgroup are shown on the 3D structure, consistent with the topology and parameter files reported in the Supporting Information.

of parameters for the doubly charged cardiolipins in the united-atom CHARMM27-UA and all-atom CHARMM36 framework. They reported the effect of cardiolipins on the order of the acyl chains and membrane thickness, which can be associated to mitochondrial membrane activity.

To date, atomistic models of all the possible protonation states of CLs have not yet been parametrized for classical molecular dynamics (MD) simulations consistent with the commonly used AMBER or CHARMM force fields. Therefore, we propose in this work an *ab initio* parametrization of CL models with different physiological protonation states, in which the phosphate groups can be either unprotonated or singly protonated. In the singly protonated CL, a proton is trapped in the bicyclic resonance structure formed by the two phosphate and hydroxyl groups (Figure 1C), for which an energy barrier as low as 4−5 kcal/mol has been estimated for the proton exchange between the phosphates.[13]

We used and tested these initial models to characterize CL-rich membrane patches and the interactions of CLs with monovalent and divalent cations. Our results are consistently validated *a posteriori* by quantum mechanics calculations and available experimental data, such as X-ray structures of proteins cocrystallized with cardiolipin molecules.

MATERIALS AND METHODS

Structural Models and Parametrization of the Cardiolipin Polar Heads. The cardiolipin headgroup possesses two phosphate groups and can therefore carry up to two negative charges. CL pK_2 (>7.5) is on the order of the physiological pH; therefore two protonation states for the cardiolipin headgroup were considered for building initial models: CLs with unprotonated phosphate groups (uCL) and singly protonated phosphate group (pCL) (Figure 1). Ideal head groups were initially built considering atoms between the phosphate groups (from atoms OA2 to OB2 in Figure 1C). Two methyl molecules were used to cap the headgroup, replacing atoms CA3 and CB3 as shown in Figure 1C.

An extensive search of the CL headgroup conformational space was carried out using Maestro.[14] A set of 991 conformers was generated. After minimization, 298 structures were clustered and ranked according to the OPLS force field[15] based energy function. The 20 most representative structures were finally extracted, and an *ab initio* geometry optimization was performed with Gaussian 09[16] at the B3LYP/6-311+G**[17] level of theory. For the CHARMM-consistent parametrization, the partial atomic charges were computed at the RHF/6-31G* level of theory and optimized to reproduce the water interaction using the Force Field Toolkit plugin.[18] For the AMBER models, the partial atomic charges were instead extracted and averaged from single point calculations at the HF/6-31G* level of theory.

Finally, the atom types and bonded force constants were extracted directly from CHARMM36[19] and general AMBER force field (GAFF)[20] parameter sets, respectively. This strategy ensures an optimal compatibility with both of the existing parametrizations. We completed the CL head models using the existing CHARMM36 parametrization for the acyl chains. The AMBER acyl parameters were instead extracted from the GLYCAM06 set.[21] These parameters, however, have not yet been finely tuned to reproduce the characteristics of acyl chains of phospholipids. The formatted topology and parameter files for MD simulations with the AMBER and CHARMM force fields are available in the Supporting Information.

Molecular Dynamics Simulations. We used molecular dynamics (MD) simulations to characterize the structural and dynamical properties of cardiolipin bilayers. In particular, tetramyristoyl cardiolipins were used for this study (Figure 1). Cardiolipins were assembled into a 60 × 60 Å^2 membrane patch composed of 50 lipids. The systems were then solvated in a 60 × 60 × 80 Å^3 water box.

Na^+ and Mg^{2+} were used to investigate the effect of monovalent and divalent cations on CL. Mg^{2+} is an abundant cation in nature and plays a central role in several biological processes. For example, Mg^{2+} is essential for the maintenance of the bacterial membrane and is required for the synthesis of cardiolipin.[22] Cardiolipins are also responsible for the Mg^{2+} inhibition of SecA.[23] NaCl or $MgCl_2$ salts were added at a concentration of ∼150 mM. A larger 200 × 200 Å^2 cardiolipin patch composed of 450 lipids was assembled to study the ions' interactions with CL when NaCl or $MgCl_2$ is mixed at a concentration of ∼150 mM.

All simulations were performed using a NAMD[24] engine, with the CHARMM36 or AMBER ff99SB force fields.[25] TIP3P water[26] parametrization was used to describe the water molecules. The periodic electrostatic interactions were computed using the particle-mesh Ewald (PME) summation

dx.doi.org/10.1021/ct300590v | J. Chem. Theory Comput. XXXX, XXX, XXX−XXX

Table 1. Biophysical Properties of Cardiolipin Membrane Patches Simulated in This Study[a]

system	force field	thickness [Å]	area per lipid [Å^2]	volume per lipid [Å^3]	diffusion coefficient [10^{-8} cm^2/s]
CDL Na^+	CHARMM	41.46 ± 1.52	90.81 ± 0.20 (30.25)	1825.43 ± 12.68	4.85 ± 0.15
CDL Mg^{2+}	CHARMM	39.53 ± 2.81	100.03 ± 0.21 (27.41)	1789.59 ± 12.41	4.65 ± 0.25
	AMBER	43.26 ± 2.6	86.45 ± 0.18 (16.16)	1859.77 ± 15.78	2.46 ± 013
CLP Na^+	CHARMM	42.67 ± 2.29	86.97 ± 0.17 (25.46)	1808.66 ± 11.54	5.26 ± 0.46
CLP Mg^{2+}	CHARMM	40.93 ± 2.63	92.83 ± 0.19 (28.16)	1795.58 ± 12.60	5.11 ± 0.18
	AMBER	44.18 ± 2.95	82.93 ± 0.14 (21.48)	1872.08 ± 16.97	2.67 ± 0.24
mixed Na^+	CHARMM	41.60 ± 2.56	90.28 ± 0.18 (24.40)	1818.10 ± 13.12	5.02 ± 0.08
mixed Mg^{2+}	CHARMM	41.42 ± 2.42	92.74 ± 0.20 (35.50)	1784.01 ± 12.70	4.54 ± 0.45
	AMBER	44.74 ± 2.96	82.54 ± 0.16 (20.61)	1833.82 ± 17.62	2.12 ± 0.11

[a]The value in parentheses for the area per lipid indicates the standard deviation measured for the patch.

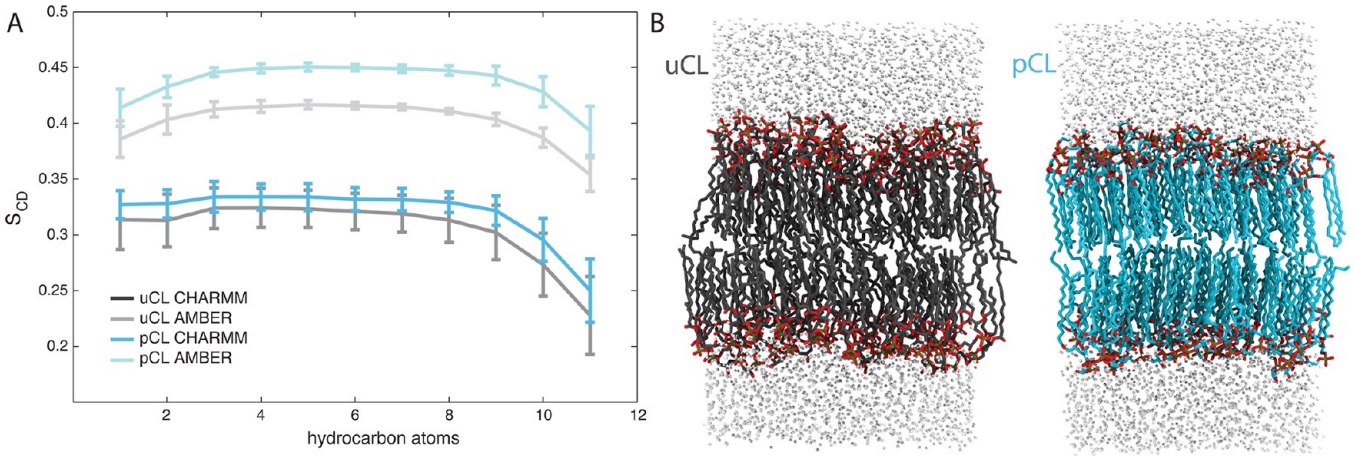

Figure 2. Biophysical properties of CL-rich membrane patches. (A) S_{CD} order parameters for pCL and uCL for both the AMBER and CHARMM parametrization. (B) Side view MD snapshots of the CL membrane systems for pCL and uCL simulated using the CHARMM force field.

with a grid spacing smaller than 1 Å. For the simulations performed with the CHARMM force field, the van der Waals interactions with the cations were modified to correct the excessive binding (NBFIX).[27] All systems were first minimized via 2000 conjugate gradient steps and then equilibrated by using a linear temperature gradient, which heated the system from 0 to 300 K in 5 ns. All systems then were equilibrated for 10 ns at 300 K. Free molecular dynamics of all equilibrated systems were performed with a 2 fs integration time step using the RATTLE algorithm applied to all bonds. Constant temperature (300 K) was imposed by using Langevin dynamics,[28] with a damping coefficient of 1.0 ps. A constant pressure of 1 atm was maintained with Langevin piston dynamics,[29] a 200 fs decay period, and a 50 fs time constant. Each simulation was run up to 300 ns after the equilibration step (Table 1). Throughout the simulations, we monitored the order parameter, area per lipid, and diffusion coefficient. We assumed that convergence was achieved when the average and the standard deviation, computed on a 20 ns sliding window, reached a plateau (i.e., always within the first 100 ns of simulation). The analyses were performed on the last 150 ns of each simulation.

***A Posteriori* Validation of the Cardiolipin Parametrization.** NWChem was used to carry out a quantum mechanics/molecular mechanics (QM/MM) microiteration-based geometry optimization.[30] A set of 50 representative bilayer structures was extracted from CHARMM and AMBER all-atom MD simulations. Head-groups (the glycerol and both phosphate groups) were then randomly selected and optimized at the QM level. The defined QM and MM regions were treated with a DFT/B3LYP[31] functional using the 6-31G*[17] basis set and Amber ff99SB force field,[20] respectively. The DFT convergence was set at 10^{-7} Hartree. The MM charges were excluded for linked MM and QM atoms. A set of 300 cycles with 500 QM and 10 000 MM iterations was performed to reach a 10^{-6} convergence.

RESULTS

CL structure and parametrization were obtained following the procedure reported in the Material and Methods section. This set of parameters is the result of an extensive conformational search of CL headgroup space, from which the most representative structures were clustered and optimized to produce a novel and consistent set of partial atomic charges. Since the pK_2 of cardiolipin (>7.5) is on the order as the physiological pH, this would imply the coexistence of different protonation states of the phosphate groups. Thus, two protonation states for cardiolipin head groups were considered in this study: CL with unprotonated phosphate groups (uCL) and a singly protonated phosphate group (pCL) (Figure 1C). To characterize the effect of the protonation, three cardiolipin bilayers were assembled. The first two systems were exclusively composed of uCL or pCL molecules. The third system was a uniform mixture of both kinds of cardiolipins. Molecular dynamics simulations were carried out for all three systems using CL parametrization consistent with the CHARMM and AMBER force fields. The subscripts "a" and "c" will be used to differentiate simulations carried out with the AMBER and CHARMM force fields, respectively (e.g., uCL_a: unprotonated

dx.doi.org/10.1021/ct300590v | J. Chem. Theory Comput. XXXX, XXX, XXX−XXX

CL with AMBER force field). CL refers to the cardiolipin independent of its protonation state.

Biophysical Characterization of the Cardiolipin Bilayer. Experimental data showed that the cardiolipin phase transition temperature is significantly higher than those corresponding to similar diacyl phospholipids.[32] Consistent with these results, a membrane patch composed exclusively of cardiolipins arranges in a gel phase conformation. To test our models, we quantified the order parameter (S_{CD}), which represents a measure of the orientation mobility of carbon−deuterium bonds that can be observed in the ^{2}H NMR experiments (Figure 2A). The computed S_{CD} profiles are in good agreement with the experimental data for the hydrophobic region of the phospholipid membrane.[33] The protonation of the phosphate group slightly affects S_{CD}; in pCL systems, the order parameter is systematically higher. The higher order parameter for CL_a indicates that the acyl chains are more parallel to the bilayer normal when using the AMBER parametrization. Mixing cardiolipins with different protonation states only marginally affected the order parameter, which remains comparable to the uniform CL patches.

Another consequence of the difference between the two parametrizations is seen by the thickness of the membranes. Membranes simulated with the AMBER force field are thicker compared to the CHARMM simulations, ∼45 Å and ∼42 Å, respectively (Table 1). At 35 °C, the thickness measured by X-ray diffraction was estimated to be ∼43 Å.[34] The acyl tails are more extended and vertical in the simulation performed with the AMBER force field and explains this difference. It was observed that MD simulations of a membrane using AMBER parameters have a tendency to favor gel over a liquid crystal phase. This may be due to the still limited testing of the force field parameters for lipids.[9a,b]

In order to estimate the variation within the membrane patch, the area per lipid was estimated using a Voronoi decomposition applied to the position of the pairs of CL phosphorus atoms.[35] The order parameters would correspond to a bilayer in gel phase, whereas the CL area per lipid is close to the one measured in the liquid crystal phase (83 Å^2 at 35 °C).[34] A similar difference has been observed for the recently reported united-atom parametrization of cardiolipins.[10c] The pCLs are significantly packed tighter than uCLs. The lipids are more tightly packed for the simulations carried out with the AMBER force field independent of the protonation state. These values are in good agreement with the ones reported by Aguayo et al.,[10c] which are the closest models reported in the literature to our parametrization. On the other hand, when mixing different protonation states, the area per lipid is comparable to the pure uCL patch. The variation of the area per lipid within a patch remained comparable for all the systems.

The diffusion coefficient of CL_c is in good agreement with the expected values for lipids from the experimental data (∼4 × 10^{-8} cm^2/s).[36] The pCL_c diffuses faster than the unprotonated cardiolipins (Table 1). The CL_a diffuses slower (1.38 ± 0.01 × 10^{-8} cm^2/s), which is consistent with the more significant gel-like conformation adopted by the acyl tails.

Exploring the Conformational Space of the Cardiolipin Polar Heads. Experimental data point to a predominant functional role of cardiolipins in several crucial cellular mechanisms, such as protein regulation, energy metabolism, and structural membrane organization. Accurately reproducing the conformation space of the polar heads is therefore essential. Currently, only limited information is available for CL headgroup geometries.

We therefore decided to characterize these properties based on our models and compare and validate the various conformers extracted from the MD simulations with the crystallographic structures of CL from PDB data, as proposed by Dahlberg and Maliniak.[10a] These structures were cocrystallized with proteins and are therefore not *per se* fully representative of a membrane bilayer. We expected however that they would sample the headgroup conformational space to some extent. A total of 91 structures formed the set of crystal structures (see Table S1 in the Supporting Information). The headgroup geometry was characterized on the basis of the interphosphate distance $d_{(PA1-PB2)}$ and the phosphate−hydroxyl angle $\theta_{(PA1-O1-PB2)}$ (Figure 3). These two variables reduce the degrees of freedom of the conformational space and describe global characteristics of the headgroup geometry.

The PDB interphosphate distance is characterized by a bimodal distribution, with a first maximum at 5.9 Å and the other at 7.0 Å (Figure 3A). In the molecular dynamics simulations, the maximum is situated at 6.8 Å and 6.7 Å for AMBER and CHARMM, respectively. The maximum for both

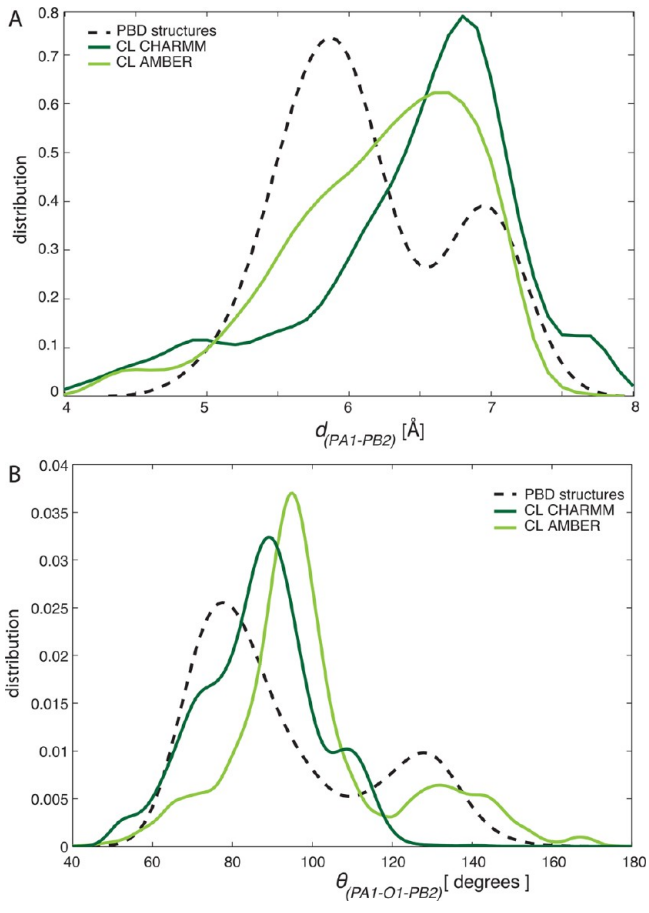

Figure 3. Conformational flexibility of the CL head groups. (A) The interphosphate distance $d_{(PA1-PB2)}$ and (B) phosphate−hydroxyl angle $\theta_{(PA1-O1-PB2)}$ of the polar heads are shown. Since the protonation state did not affect these variables, the simulations are averaged depending on the force field used. The relative quantities extracted from CLs crystallized in the PDB structures are shown with dashed lines (see the SI for the exhaustive list of the protein complexes used for this analysis).

dx.doi.org/10.1021/ct300590v | J. Chem. Theory Comput. XXXX, XXX, XXX−XXX

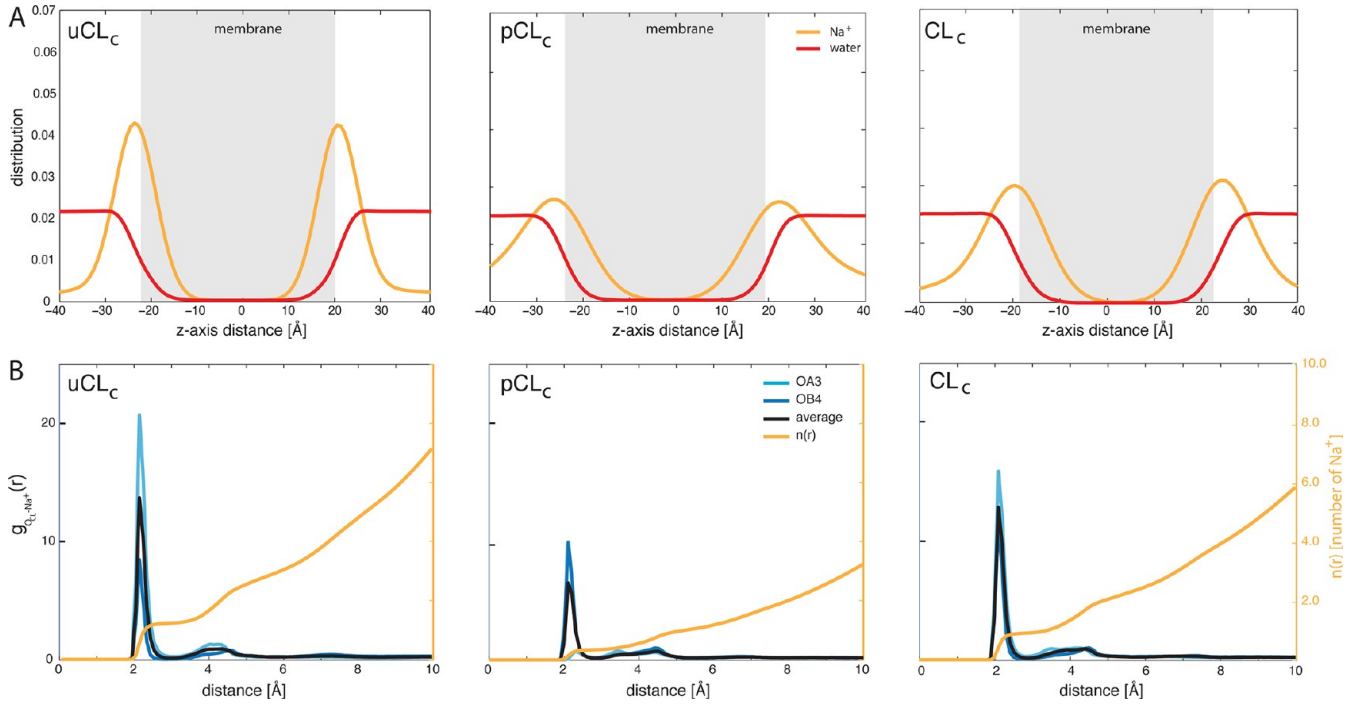

Figure 4. Cardiolipin interactions with sodium. (A) Distribution of Na^+ (in orange) and water molecules (in red) along the z axis normal to the membrane surface. From left to right, data for the uCL, pCL, and CL (mixed uCL/pCL) systems are reported for the CHARMM force field. (B) Radial distribution function $g(r)$ and coordination number $n(r)$ (in orange) for Na^+ with respect to CL phosphate oxygen atoms for simulations carried out with the CHARMM force field.

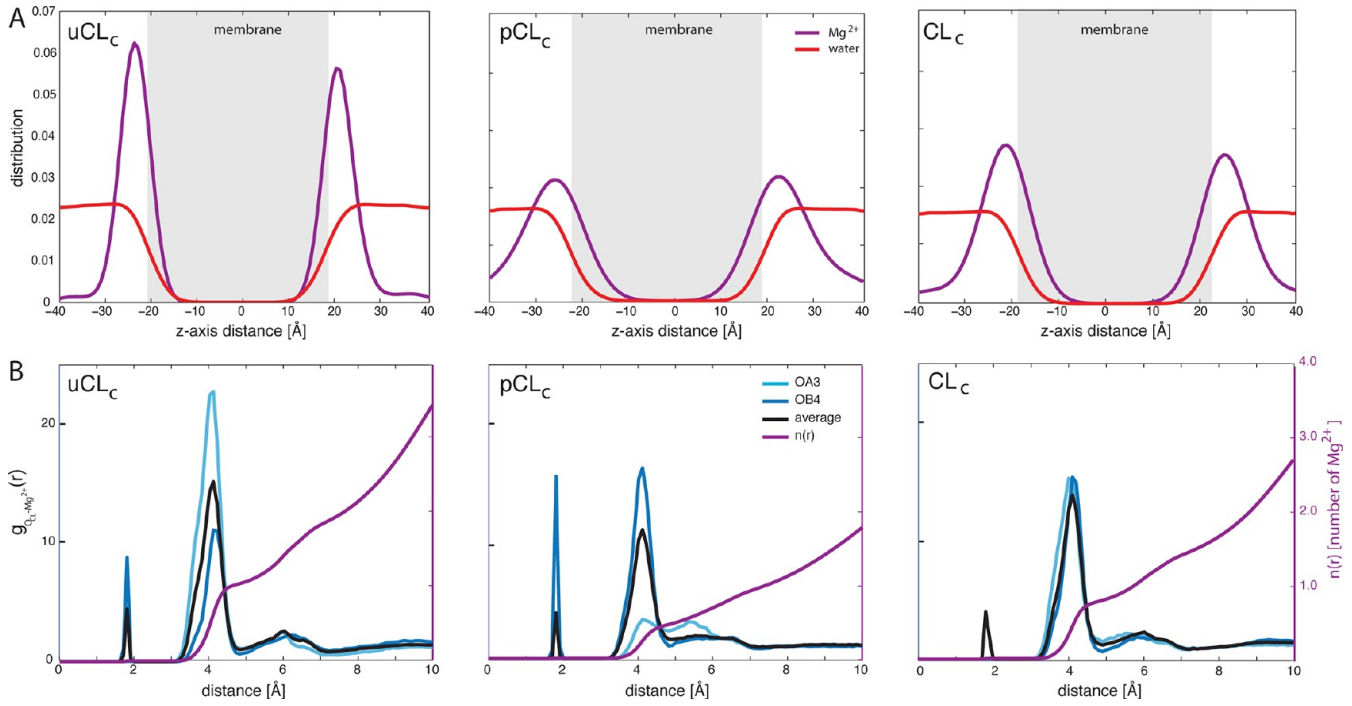

Figure 5. Cardiolipin interactions with magnesium. (A) Distribution of Mg^{2+} (in purple) and water molecules (in red) along the z axis normal to the membrane surface. From left to right, data for the uCL, pCL, and CL (mixed uCL/pCL) systems are reported for the CHARMM force field. (B) Radial distribution function $g(r)$ and coordination number $n(r)$ (in purple) for Mg^{2+} with respect to phosphate oxygen atoms for simulations carried out with the CHARMM force field (see results for AMBER force field in the SI).

force fields is closer to the second experimental maximum (7.0 Å). CHARMM covers more uniformly the conformational space. Despite this shift, the conformation space explored by both models is in good agreement with these experimental data, even though the PDB structures do not represent bilayer structures. The protonation state does not significantly influence these distributions. The angle distribution is also bimodal (maxima at 78 and 128 degrees). CHARMM-based

dx.doi.org/10.1021/ct300590v | J. Chem. Theory Comput. XXXX, XXX, XXX−XXX

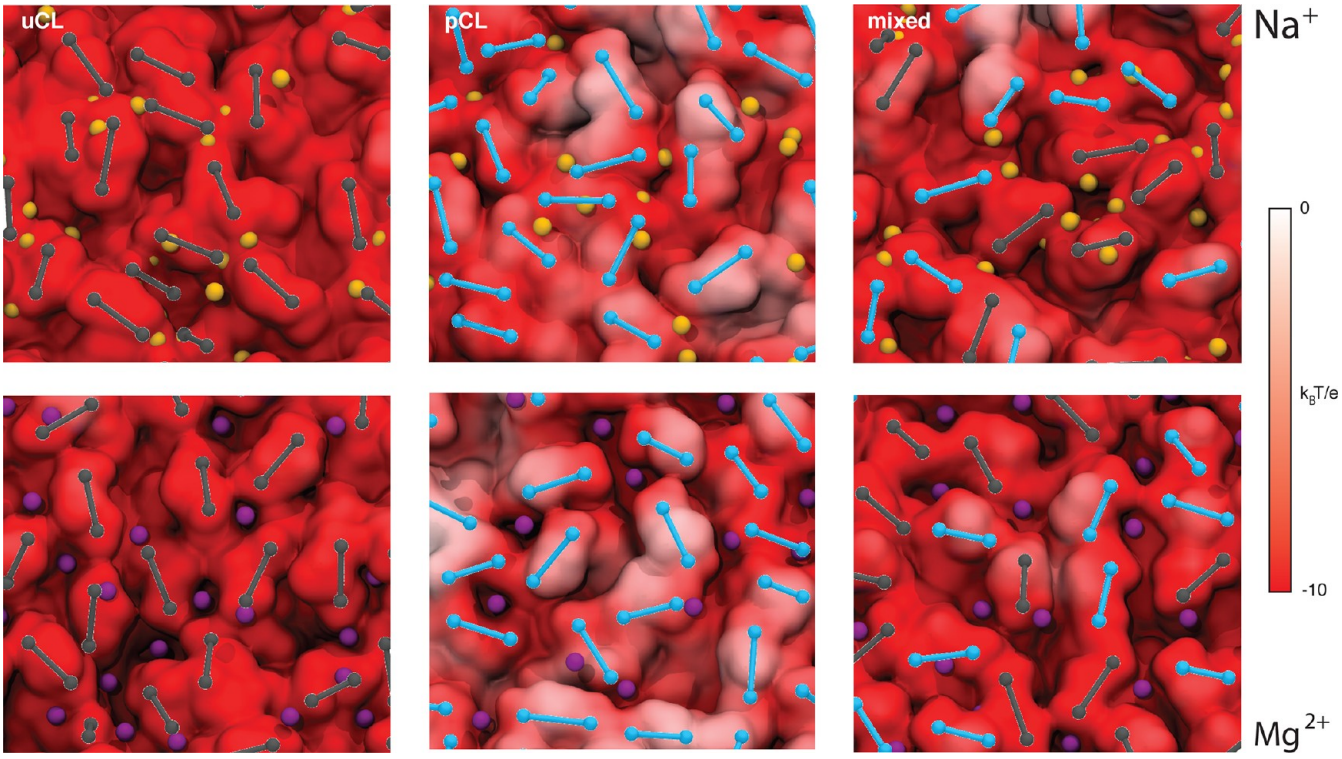

Figure 6. Electrostatic properties of the CL-rich membrane surface. The electrostatic potential of the cardiolipin membrane surface was computed with APBS[45] and plotted on the molecular surface of the CL membrane. For the sake of clarity, the uCL molecules are topologically identified with gray balls representing the phosphorus atoms connected by sticks. Similarly, pCL moieties are in blue. Na^+ and Mg^{2+} cations are shown as orange and purple spheres, respectively.

models show a single mode distribution, which largely overlaps the PDB global maxima. The principal mode for the AMBER force field is shifted (95 degrees), but the distribution is bimodal with a second mode closer to PDB (132°; Figure 3B).

In order to further quantify the accuracy of the atomic partial charges and dihedral parameters derived for the headgroup, a hybrid quantum mechanics/molecular mechanics (QM/MM) geometry optimization was carried out. A set of 50 membrane bilayer structures was extracted from the MD simulations. Single CL molecules in the patch were randomly selected to be geometrically optimized at the QM/MM level. The refined structures were in good agreement with the MD headgroup conformation (RMSD 0.13 ± 0.03 Å). The interphosphate distance and phosphate−hydroxyl angle varied only slightly (0.08 ± 0.13 Å and 0.39 ± 3.00°, respectively). The angles and dihedrals of the bonded atoms of the headgroup remained constant between the MM and QM structures with a variation under 10%.

Therefore, the reasonably good conformational overlap with available crystallized structures of CLs and the limited variation of CL geometries relaxed at a higher level of theory support a good structural robustness of the force field parameters derived here for MD simulations.

Cardiolipin Interactions with Cations. Cations are known to be crucial for the structural and functional integrity of cell membranes. The anionic nature of cardiolipins makes them a major binding site for cations, or positively charged species (e.g., AMPs). We therefore analyzed the distribution along the z axis normal to the membrane surface and the radial distribution function of Na^+ and Mg^{2+} with respect to CL lipids (Figures 4 and 5). A larger patch (200 × 200 $Å^2$) was also used to study the combined effect of Na^+ and Mg^{2+}. Since at this stage, the CHARMM model seems to better capture the physical properties of the membrane, the results for this model will be presented in more detail (additional results for AMBER models are reported in the Supporting Information).

In the unprotonated system, 90% of the Na^+ and 85% of the Mg^{2+} are localized within 4 Å from the membrane surface (Figures 4A and 5A, respectively). The protonation leads to a broadening of the distribution, reducing to 55% the number of Na^+ and 76% the number of Mg^{2+} within 4 Å from the surface. It is of interest to note that this proportion increases to ∼89% for both cations when interacting with the mixed protonation state bilayer. Consistent with the experimental data, the phosphate groups constitute the main binding site for cations. On one hand, Na^+ cations are partially buried in the membrane (Figure 4A). These cations interact directly with the CL phosphate oxygen atoms (i.e., OA3 and OB4), corresponding to the first peak in the radial distribution function (Figure 4B). Several Na^+ cations interact with a single cardiolipin molecule (Figure S2, for a representative CL−Na^+ conformation). On the other hand, despite a few Mg^{2+} cations forming direct interactions with the CL phosphate oxygen atoms, the main solvation structure indicates that CL−divalent cation interactions are water mediated. The most relevant peak found at ∼4 Å corresponds to Mg^{2+} surrounded by their first solvation shell in an octahedral conformation, with water hydrogen atoms pointing toward the phosphate group or the bulk. The peak at ∼6 Å mainly represents the other phosphate group of a cardiolipin, which interacts with a cation (see Figure S2 for a representative CL−Mg^{2+} conformation). For the unprotonated systems (uCL), each phosphate is able to interact globally with one cation in the first shell, whereas when one phosphate is protonated (pCL systems), the cation occupancy is nearly half

dx.doi.org/10.1021/ct300590v | J. Chem. Theory Comput. XXXX, XXX, XXX−XXX

(pCL system in Figure 5B and Figure S1A). When the uCL and pCL moieties are mixed, the phosphate−cation interactions are mixed as well, showing an improved ability, as compared to the pCL system, to globally attract cations close to the membrane surface. The area per lipid decreases significantly in the presence of Na^+ in the pure protonated or unprotonated cardiolipin patches (Table 1). The order parameters, however, are not modified and, therefore, do not contribute to this difference in the area per lipid. The effect of cations on the area per lipid is only marginal in the mixed protonated CL bilayer.

The different CL protonation states produce a different electrostatic signature for the membrane surface, which is directly related to the CL ability to interact with cations and possibly other proteins and/or phospholipids. As expected, the uCL membrane surface displays a distinct strong negative charge, whereas the surface for pCL is less charged, which is consistent with the normal distribution of cations at the membrane (Figure 6). Cations are localized in contact with the most highly charged regions. Complex and intricate networks involving several cardiolipins were observed. In the presence of monovalent cations, the cardiolipins form a very tight network trapping up to three Na^+'s per CL (Figure S2). In contrast, the cardiolipins form pockets composed of up to three lipids, which are able to trap a Mg^{2+} cation (Figure S2).

When Na^+ and Mg^{2+} cations are both present in a mixed protonated CL bilayer, more cations are simultaneously interacting with at least one protonated and one unprotonated cardiolipin. There are up to twice as many Na^+'s as Mg^{2+}'s interacting only with uCL molecules and at the interface of the protonated and unprotonated cardiolipins (Figure 7A). In contrast, the pCL interacts almost equally with both cations. The radial distribution of Mg^{2+} within 6 Å of the membrane surface corresponds to the one expected for molecules which do not interact (Figure 7B). This indicates a random distribution of Mg^{2+} on the membrane surface. In contrast, the Mg^{2+} radial distribution function with respect to Na^+ shows a clear peak at 5 Å, which corresponds to Mg^{2+} and Na^+ cation interacting simultaneously with the same cardiolipin molecules. The cardiolipins impose a structural order to the Na^+ cations, via their direct interaction with the phosphate group. The interaction with the Na^+ packs tighter the CL head groups, allowing a Mg^{2+} cation to be trapped above the Na^+ (Figure S2). On average, such an interaction involves a single Mg^{2+} and Na^+ cation and represents ∼5% of the Mg^{2+} localized close to the membrane surface.

DISCUSSION

Cardiolipins represent a unique anionic lipid species, which is only present in bacterial and mitochondrial membranes, and plays a key role in several cellular functions. To date, only limited information concerning CL physicochemical properties is available. We therefore built and parametrized cardiolipin models for the commonly used AMBER and CHARMM force fields, to allow a further investigation of their fundamental role through molecular dynamics simulations. Since the pK_2 of CLs is close to the physiological pH, two protonation states for the phosphate groups are likely to be present under normal conditions (an unprotonated (uCL) and the singly protonated (pCL) CL conformation); their properties, mutual interactions, and interactions with cations are characterized for the first time in this study.

Our model accurately reproduces the lateral diffusion coefficient and the area per lipid expected for lipid bilayers,

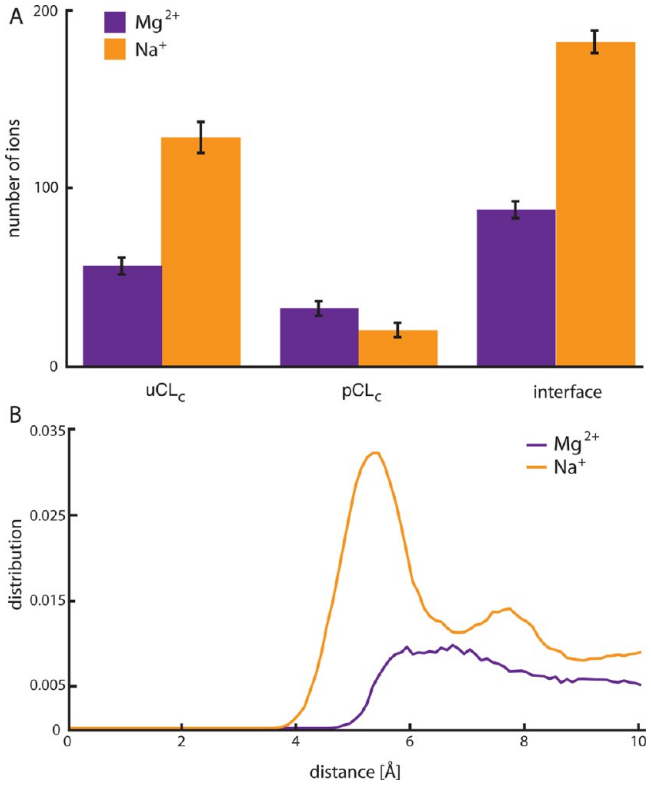

Figure 7. Cardiolipins in the presence of sodium and magnesium cations. (A) Number of cations interacting with only uCL molecules, pCL molecules, and with at least one uCL and one pCL molecule (interface). (B) Radial distribution function $g(r)$ for Mg^{2+} with respect to Mg^{2+} and Na^+.

with the CHARMM parametrization better capturing the physical properties of the membrane. This difference can be explained by the fact that AMBER acyl parameters have not yet been extensively tested and optimized for lipid bilayers. Recently, a new set of parameters for the acyl chains has been proposed.[37] Coupling these new parameters to our AMBER models of the headgroup can be a good starting point for further development.

The asymmetry created by the protonation of the phosphate groups leads to a modification of the area per lipid (Table 1). Consistent with our observation, Khalifat et al. studied the effect of pH on the packing of the cardiolipin-containing bilayer[38] and proposed that the change in the area per lipid is the driving force for membrane shape instability. Moreover, the presence of cardiolipin domains and their pH-dependent packing could function as a proton sink. It has been suggested in fact that cardiolipins stabilize the proton gradient across the membrane necessary for ATP synthesis.[39] Since cardiolipins are also associated with the proton uptake pathway in the cytochrome bc1 complex, they may play a role in proton conduction.[40] The proposed models will therefore allow investigation of the effect of CL protonation on these systems at the molecular mechanics level.

A PDB data-mining was used to characterize the conformation space of cardiolipins. Even though cardiolipins present in the PDB cocrystallized with proteins have a low statistical weight, and are not entirely representative of a bilayer conformation, the interphosphate distance and hydroxyl−phosphate angle measured from MD simulations nicely overlap with this distribution. This implies that the conformational

dx.doi.org/10.1021/ct300590v | J. Chem. Theory Comput. XXXX, XXX, XXX−XXX

space accessible to CL molecules forming a bilayer is greater, but largely overlaps with the one representing the interaction of CL with protein complexes. CLs thus can smoothly transition from the membrane phase to interacting with proteins without a specific contrasting conformational rearrangement. The higher CL binding affinity for specific protein regions would therefore be the only main driving force for CL−protein interactions.

It is known that cations, especially divalent, influence the physicochemical properties of cardiolipins (e.g., transition temperature, nonlamellar macroscopic phases).[32] The CL surface displays a net negative charge attracting the cations to the membrane surface. Consistent with experimental evidence, we observe that cations interact primarily with CL phosphate groups.[41] While the monovalent cation interacts directly with the oxygen atoms, only a few divalent cations are trapped in the first solvation shell of the phosphate. Their main mode of interaction is through water-mediated bridges with CL phosphates. Nonetheless, CL-rich membranes are able to attract a high concentration of cations from the bulk. The cations neutralize up to 96% of the membrane surface charge. Thus, the binding of the cations could modify the membrane surface electrostatic potential. Using NMR, Macdonald and Seelig[42] showed that the binding of Ca^{2+} is predominantly due to electrostatic effects, rather than to the intrinsic affinity with CLs. Furthermore, in addition to the screening effect, interactions with cations shape the complex network of cardiolipins, which form negatively charged cavities where the Na^{+} and Mg^{2+} cations are trapped.

In a bacteria membrane, phosphatidylglycerol (PG) and CL are the major contributors to the membrane surface negative charge. Antimicrobial peptides (AMPs), which are part of the immune system, are characterized by a cationic amphiphilic nature, mirroring the properties of the bacterial membrane. During critical phases of an infection, such as cell division, the bacterial membranes are enriched in cardiolipins at the expense of PG.[43] Cardiolipins with their mixed protonation conformations could therefore constitute a key target for the AMPs. It has been shown in fact that cardiolipins and divalent cations modulate the binding of antimicrobial peptides to Gram-positive bacteria.[44]

In conclusion, the proposed models of cardiolipins have been shown to be reliable and robust and can reproduce the biophysical properties of cardiolipin-rich membrane portions. The availability of parametrized models accounting for multiple protonation states present under physiological conditions will permit the building of more realistic systems representative of the bacterial and mitochondrial membrane. This will allow the gaining of insight, through molecular simulations, into the biophysical properties of different membrane mixtures exposed to different environmental conditions, such as cation concentrations, AMPs stress, and protein complex interactions.

■ ASSOCIATED CONTENT

Supporting Information

Three sections with two figures, one table, and formatted files for CL parameters and topologies are available. This information is available free of charge via Internet at http://pubs.acs.org/.

■ AUTHOR INFORMATION

Corresponding Author

*E-mail: matteo.dalperaro@epfl.ch. Phone: +41 21 693 1861.

Author Contributions

†These authors contributed equally to this work

Notes

The authors declare no competing financial interest.

■ ACKNOWLEDGMENTS

This research was supported by the Swiss National Science Foundation (grant number 200021_135450) and by CPU allocation grants from the Swiss National Supercomputing Centre (CSCS), the Center for Advance Modeling Science (CADMOS), and the Partnership for Advanced Computing in Europe (PRACE).

■ REFERENCES

(1) Matsumoto, K.; Kusaka, J.; Nishibori, A.; Hara, H. Lipid domains in bacterial membranes. *Mol. Microbiol.* **2006**, *61*, 1110−1117.

(2) (a) Lucero, H. A.; Robbins, P. W. Lipid rafts-protein association and the regulation of protein activity. *Arch. Biochem. Biophys.* **2004**, *426*, 208−224. (b) Wisniewska, A.; Draus, J.; Subczynski, W. K. Is a fluid-mosaic model of biological membranes fully relevant? Studies on lipid organization in model and biological membranes. *Cell. Mol. Biol. Lett.* **2003**, *8*, 147−160.

(3) van Meer, G.; Voelker, D. R.; Feigenson, G. W. Membrane lipids: where they are and how they behave. *Nat. Rev. Mol. Cell Biol.* **2008**, *9*, 112−124.

(4) (a) Hoch, F. L. Cardiolipins and Biomembrane Function. *Biochim. Biophys. Acta* **1992**, *1113*, 71−133. (b) Hoch, F. L. Minireview: Cardiolipins and mitochondrial proton-selective leakage. *J. Bioenerg. Biomembr.* **1998**, *30*, 511−532.

(5) Kates, M.; Syz, J. Y.; Gosser, D.; Haines, T. H. Ph-Dissociation Characteristics of Cardiolipin and Its 2'-Deoxy Analog. *Lipids* **1993**, *28*, 877−882.

(6) Nichols-Smith, S.; Kuhl, T. Electrostatic interactions between model mitochondrial membranes. *Colloids Surf., B* **2005**, *41*, 121−7.

(7) Pierucci, O. Phospholipid-Synthesis during the Cell-Division Cycle of Escherichia-Coli. *J. Bacteriol.* **1979**, *138*, 453−460.

(8) Houtkooper, R. H.; Vaz, F. M. Cardiolipin, the heart of mitochondrial metabolism. *Cell. Mol. Life Sci.* **2008**, *65*, 2493−2506.

(9) (a) Egberts, E.; Marrink, S. J.; Berendsen, H. J. C. Molecular-Dynamics Simulation of a Phospholipid Membrane. *Eur. Biophys. J. Biophys.* **1994**, *22*, 423−436. (b) Heller, H.; Schaefer, M.; Schulten, K. Molecular-Dynamics Simulation of a Bilayer of 200 Lipids in the Gel and in the Liquid-Crystal Phases. *J. Phys. Chem.* **1993**, *97*, 8343−8360. (c) Bandyopadhyay, S.; Shelley, J. C.; Klein, M. L. Molecular dynamics study of the effect of surfactant on a biomembrane. *J. Phys. Chem. B* **2001**, *105*, 5979−5986.

(10) (a) Dahlberg, M.; Maliniak, A. Molecular dynamics simulations of cardiolipin bilayers. *J. Phys. Chem. B* **2008**, *112*, 11655−11663. (b) Dahlberg, M. Polymorphic phase behavior of cardiolipin derivatives studied by coarse-grained molecular dynamics. *J. Phys. Chem. B* **2007**, *111*, 7194−7200. (c) Aguayo, D.; Gonzalez-Nilo, F. D.; Chipot, C. J. Insight into the properties of cardiolipin containing bilayers from molecular dynamics simulations, using a hybrid all-atom/united-atom force field. *J. Chem. Theory Comput.* **2012**; (d) Murzyn, K.; Rog, T.; Pasenkiewicz-Gierula, M. Phosphatidylethanolamine-phosphatidylglycerol bilayer as a model of the inner bacterial membrane. *Biophys. J.* **2005**, *88*, 1091−1103.

(11) Rog, T.; Martinez-Seara, H.; Munck, N.; Oresic, M.; Karttunen, M.; Vattulainen, I. Role of Cardiolipins in the Inner Mitochondrial Membrane: Insight Gained through Atom-Scale Simulations. *J. Phys. Chem. B* **2009**, *113*, 3413−3422.

(12) Murzyn, K.; Pasenkiewicz-Gierula, M. Construction and optimization of a computer model for a bacterial membrane. *Acta Biochim. Pol.* **1999**, *46*, 631−639.

(13) Dahlberg, M.; Marini, A.; Mennucci, B.; Maliniak, A. Quantum chemical modeling of the cardiolipin headgroup. *J. Phys. Chem. A* **2010**, *114*, 4375−87.

(14) *Maestro*, version 8.5; Schroedinger, LLC: New York, 2010.
(15) Jorgensen, W. L.; Maxwell, D. S.; Tirado Rives, J. Development and testing of the OPLS all-atom force field on conformational energetics and properties of organic liquids. *J. Am. Chem. Soc.* **1996**, *118*, 11225−11236.
(16) Frisch, M.; Trucks, G.; Schlegel, H.; Scuseria, G.; Robb, M.; Cheeseman, J.; Scalmani, G.; Barone, V.; Mennucci, B.; Petersson, G. *Gaussian-09*, Rev. A. 1; Gaussian. Inc.: Wallingford, CT, 2009.
(17) Raghavachari, K. Perspective on "Density functional thermochemistry. III. The role of exact exchange" - Becke AD (1993) J Chem Phys 98:5648−52. *Theor. Chem. Acc.* **2000**, *103*, 361−363.
(18) Mayne, C. G.; Tajkhorshid, E.; Gumbart, J. Force Field Toolkit Plugin. www.ks.uiuc.edu/Research/vmd/plugins/fftk (accessed Dec. 2012).
(19) Klauda, J. B.; Venable, R. M.; Freites, J. A.; O'Connor, J. W.; Tobias, D. J.; Mondragon-Ramirez, C.; Vorobyov, I.; MacKerell, A. D.; Pastor, R. W. Update of the CHARMM All-Atom Additive Force Field for Lipids: Validation on Six Lipid Types. *J. Phys. Chem. B* **2010**, *114*, 7830−7843.
(20) Hornak, V.; Abel, R.; Okur, A.; Strockbine, B.; Roitberg, A.; Simmerling, C. Comparison of multiple amber force fields and development of improved protein backbone parameters. *Proteins* **2006**, *65*, 712−725.
(21) Tessier, M. B.; DeMarco, M. L.; Yongye, A. B.; Woods, R. J. Extension of the GLYCAM06 biomolecular force field to lipids, lipid bilayers and glycolipids. *Mol. Simul.* **2008**, *34*, 349−363.
(22) Tunaitis, E.; Cronan, J. E., Jr. Characterization of the cardiolipin synthetase activity of Escherichia coli envelopes. *Arch. Biochem. Biophys.* **1973**, *155*, 420−7.
(23) Gold, V. A.; Robson, A.; Clarke, A. R.; Collinson, I. Allosteric regulation of SecA: magnesium-mediated control of conformation and activity. *J. Biol. Chem.* **2007**, *282*, 17424−32.
(24) Phillips, J. C.; Braun, R.; Wang, W.; Gumbart, J.; Tajkhorshid, E.; Villa, E.; Chipot, C.; Skeel, R. D.; Kale, L.; Schulten, K. Scalable molecular dynamics with NAMD. *J. Comput. Chem.* **2005**, *26*, 1781−1802.
(25) Brooks, B. R.; Brooks, C. L., 3rd; Mackerell, A. D., Jr.; Nilsson, L.; Petrella, R. J.; Roux, B.; Won, Y.; Archontis, G.; Bartels, C.; Boresch, S.; Caflisch, A.; Caves, L.; Cui, Q.; Dinner, A. R.; Feig, M.; Fischer, S.; Gao, J.; Hodoscek, M.; Im, W.; Kuczera, K.; Lazaridis, T.; Ma, J.; Ovchinnikov, V.; Paci, E.; Pastor, R. W.; Post, C. B.; Pu, J. Z.; Schaefer, M.; Tidor, B.; Venable, R. M.; Woodcock, H. L.; Wu, X.; Yang, W.; York, D. M.; Karplus, M. CHARMM: the biomolecular simulation program. *J. Comput. Chem.* **2009**, *30*, 1545−614.
(26) Jorgensen, W. L.; Chandrasekhar, J.; Madura, J. D.; Impey, R. W.; Klein, M. L. Comparison of simple potential functions for simulating liquid water. *J. Chem. Phys.* **1983**, *79*, 926.
(27) (a) Mayaan, E.; Moser, A.; MacKerell, A. D., Jr.; York, D. M. CHARMM force field parameters for simulation of reactive intermediates in native and thio-substituted ribozymes. *J. Comput. Chem.* **2007**, *28*, 495−507. (b) Noskov, S. Y.; Berneche, S.; Roux, B. Control of ion selectivity in potassium channels by electrostatic and dynamic properties of carbonyl ligands. *Nature* **2004**, *431*, 830−4.
(28) Brunger, A.; Brooks, C. L. Stochastic boundary conditions for molecular dynamics simulations of ST2 water. *Chem. Phys. Lett.* **1984**, *105*, 495−500.
(29) Feller, S. E.; Zhang, Y.; Pastor, R. W.; Brooks, B. R. Constant pressure molecular dynamics simulation: the Langevin piston method. *J. Chem. Phys.* **1995**, *103*, 4613.
(30) Valiev, M.; Bylaska, E. J.; Govind, N.; Kowalski, K.; Straatsma, T. P.; Van Dam, H. J. J.; Wang, D.; Nieplocha, J.; Apra, E.; Windus, T. L.; de Jong, W. NWChem: A comprehensive and scalable open-source solution for large scale molecular simulations. *Comput. Phys. Commun.* **2010**, *181*, 1477−1489.
(31) Wadt, W. R.; Hay, P. J. Ab initio effective core potentials for molecular calculations. Potentials for main group elements Na to Bi. *J. Chem. Phys.* **1985**, *82*, 284.
(32) Lewis, R. N. A. H.; McElhaney, R. N. The physicochemical properties of cardiolipin bilayers and cardiolipin-containing lipid membranes. *Biochim. Biophys. Acta, Biomembr.* **2009**, *1788*, 2069−2079.
(33) Vermeer, L. S.; de Groot, B. L.; Reat, V.; Milon, A.; Czaplicki, J. Acyl chain order parameter profiles in phospholipid bilayers: computation from molecular dynamics simulations and comparison with 2H NMR experiments. *Eur. Biophys. J.* **2007**, *36*, 919−31.
(34) Lewis, R. N. A. H.; Zweytick, D.; Pabst, G.; Lohner, K.; McElhaney, R. N. Calorimetric, X-ray diffraction, and spectroscopic studies of the thermotropic phase behavior and organization of tetramyristoyl cardiolipin membranes. *Biophys. J.* **2007**, *92*, 3166−3177.
(35) Shinoda, W.; Okazaki, S. A Voronoi analysis of lipid area fluctuation in a bilayer. *J. Chem. Phys.* **1998**, *109*, 1517−1521.
(36) Bockmann, R. A.; Hac, A.; Heimburg, T.; Grubmuller, H. Effect of sodium chloride on a lipid bilayer. *Biophys. J.* **2003**, *85*, 1647−55.
(37) Dickson, C. J.; Rosso, L.; Betz, R. M.; Walker, R. C.; Gould, I. R. GAFFlipid: a General Amber Force Field for the accurate molecular dynamics simulation of phospholipid. *Soft Matter* **2012**, *8*, 9617−9627.
(38) Khalifat, N.; Fournier, J. B.; Angelova, M. I.; Puff, N. Lipid packing variations induced by pH in cardiolipin-containing bilayers: the driving force for the cristae-like shape instability. *Biochim. Biophys. Acta* **2011**, *1808*, 2724−33.
(39) Haiens, T. H.; Dencher, N. A. Cardiolipin: a proton trap for oxidative phosphorylation. *FEBS Lett.* **2002**, *528*, 35−39.
(40) Lange, C.; Nett, J. H.; Trumpower, B. L.; Hunte, C. Specific roles of protein-phospholipid interactions in the yeast cytochrome bc1 complex structure. *EMBO J.* **2001**, *20*, 6591−600.
(41) (a) Tatulian, S. A. Binding of Alkaline-Earth Metal-Cations and Some Anions to Phosphatidylcholine Liposomes. *Eur. J. Biochem.* **1987**, *170*, 413−420. (b) Huster, D.; Arnold, K.; Gawrisch, K. Strength of Ca2+ binding to retinal lipid membranes: Consequences for lipid organization. *Biophys. J.* **2000**, *78*, 3011−3018. (c) Garidel, P.; Blume, A.; Hubner, W. A Fourier transform infrared spectroscopic study of the interaction of alkaline earth cations with the negatively charged phospholipid 1,2-dimyristoyl-sn-glycero-3-phosphoglycerol. *Biochim. Biophys. Acta, Biomembr.* **2000**, *1466*, 245−259.
(42) Macdonald, P. M.; Seelig, J. Calcium-Binding to Mixed Cardiolipin Phosphatidylcholine Bilayers as Studied by Deuterium Nuclear-Magnetic-Resonance. *Biochemistry* **1987**, *26*, 6292−6298.
(43) Koppelman, C. M.; Den Blaauwen, T.; Duursma, M. C.; Heeren, R. M. A.; Nanninga, N. Escherichia coli minicell membranes are enriched in cardiolipin. *J. Bacteriol.* **2001**, *183*, 6144−6147.
(44) Som, A.; Yang, L.; Wong, G. C.; Tew, G. N. Divalent metal ion triggered activity of a synthetic antimicrobial in cardiolipin membranes. *J. Am. Chem. Soc.* **2009**, *131*, 15102−3.
(45) Baker, N. A.; Sept, D.; Joseph, S.; Holst, M. J.; McCammon, J. A. Electrostatics of nanosystems: Application to microtubules and the ribosome. *Proc. Natl. Acad. Sci. U. S. A.* **2001**, *98*, 10037−10041.